ISSN: 2754-4915

Journal of Material Sciences & Manufacturing Research

SCIENTIFIC Research and Community

Research Article

Open Access

Optimizing Spin-Coat Speed for Fabrication of P3HT: PCBM Solar Cells

Tirukoti Mounika[1,2], Shiddappa L Belagali[1], Inderpreet Singh[2], Nimmi Singh[3]*, Kuldeep Kumar[3] and P. Arun[2]

[1]Environmental Chemistry Laboratory, Department of Studies in Environmental Science, University of Mysore, Manasagangothri, Mysore, Karnataka, India

[2]Department of Electronics, SGTB Khalsa College, University of Delhi, Delhi, India

[3]Department of Physics, SGTB Khalsa College, University of Delhi, Delhi, India

ABSTRACT

The effect of spin speed on the orientation of the conjugated polymer chains becomes a matter of concern while fabricating bulk heterojunction devices such as solar cells. The stability and performance strongly depend on the intertwining of the two molecules that form the bulk heterojunctions. In the case of P3HT: PCBM, it is the long chains of P3HT that encompasses the PCBM molecules. This work investigates the fabricating conditions of Poly (3-hexylthiophene) (P3HT) on the glass substrates in terms of spin coating speeds to obtain favourable geometry of P3HT. For this purpose, three different samples were prepared, keeping spin rate as 6850, 8150 and 9700 rpm, respectively. It was observed that at high spin rates, a large centrifugal force acts upon polymer chains, unfolding them into highly oriented structures. These P3HT chains are free from twists, kinks and are not intermingled. The results of the present work advocate fabricating P3HT: PCBM films at spin speeds less than 6850 rpm.

***Corresponding author**

Nimmi Singh, Department of Physics, SGTB Khalsa College, University of Delhi, Delhi, India.

Received: February 01, 2024; **Accepted:** February 16, 2024; **Published:** February 23, 2024

Keywords: Polymer, Thin Films, Crystallization, Orientated Growth

Introduction

Photovoltaics, a branch of Physical Sciences, is dedicated towards the development of solar cell structures that can efficiently capture sunlight and convert it into electricity. In this field, Silicon has been extensively used in the commercialization of stable solar cells. However, the fabrication of such devices pollutes the environment and lacks flexibility. This means a serious limitation on surfaces that solar cells can be attached and in their transportation. Thus, there is a requirement for alternatives to Silicon that are not only efficient but are flexible and do not pollute the environment as well.

The possibility of developing flexible electronic devices and displays using conjugated polymers has drawn the attention of researches working worldwide [1-11]. This is due to the fact that conjugated polymers possess a wonderful combination of semiconductor-like optical and electrical properties along with mechanical strength similar to that of plastic [12-16]. The most important advantage of polymers over inorganic semiconductors is that they can be doped either as p- or n-type using simple oxidation or reduction reactions, respectively [17,18]. Also, purification of polymers is not required to the same level as it is required for inorganic semiconductors. Their ability to dissolve in a variety of organic solvents makes it possible to fabricate electronic devices using simple solution processing techniques such as spin coating, doctor blading and inkjet printing [19-23]. An added advantage of this is that all these processes are also environment friendly.

Poly(3-hexylthiophene), or P3HT, as it is more popularly referred to, is a well-known conjugated polymer used as a photo-active layer in solar cells. In the past two decade or so, P3HT has become a very popular choice for fabrication of bulk heterojunction solar-cells with Phenyl-C61-butyric acid methyl ester (PCBM) acceptor moelcules [24-29]. P3HT is known to have an absorption peak at 510 nm, that is suitable for efficient capture of light from the sun to be converted into electrical energy. In addition to this, it also has a high absorption coefficient in the visible wavelength region [30-35]. Hence, a large number of excitons are generated in the P3HT polymer chains when illuminated by sunlight.

However, these excitons have tendency to decay rapidly and the polymer films require acceptor molecules having high electron affinity. These molecules should be able to dissociate the photogenerated exciton into individual holes and electrons before their radiative decay. The so dissociated electrons are then dragged by the acceptor molecules and transported to cathode. The holes remaining in polymer, hops through polymer chains and move towards anode. For this process to occur efficiently the acceptor molecules should be homogeneously distributed with in the polymer film.

The P3HT polymers have long chain molecules which are highly flexible and form random coils [36,37]. This coiling is anticipated to hold or "imprison" PCBM molecules to establish

a perfect bulk heterojunction. Yet it is observed that the device efficiency deteriorates with time [38-40]. Which would mean either PCBM molecules somehow escape from the P3HT coils or P3HT molecules coiling did not occur, suggesting growth parameters were not optimised. While there are many publications on P3HT bulk heterojunction solar cells, a few focus on effect of fabrication conditions on the quality of the film as in ability to control the chain bending and twisting, etc. In the present work, we have deposited P3HT films on glass substrates using spin coating and studied the effect of spin speed on the orientation of the polymer chains. The novelty of the conducted work is that it shows a relationship between the ordering/ alignment of polymer chains and spin rate. This work can be used to optimize the spin rate while fabricating polymer based photovoltaic strictures for the development of stable solar cells.

Experimental Details

The P3HT polymer used in this study was procured from Sigma-Aldrich Chemicals Private Limited with an AR grade of > 99.5% purity. It was dispersed in chlorobenzene (10 mg/ml) and mixed thoroughly with the help of ultrasonicator for 2-hours until a homogeneous solution was obtained. This solution was then used for deposition of the films on clean glass substrates by spin coating method. To study the effect of spin-rate, three different films were coated by varying the rpm of the spinner. For this purpose, the DC motor's excitation voltage is varied and spin speed was measured using a tachometer. To avoid ambiguity, films have been named as per the rpm at which the samples were grown.

The crystallinity of the films was characterised using Rigaku Ultima IV X-Ray diffractometer, while their optical behavior such as absorbance and Photoluminescence (PL) were studied using Shimadzu's UV-visible spectrophotometer (Model UV-2540) and Shimadzu's Spectrofluorophotometer Model RF 5301PC, respectively. The surface roughness and thickness of the grown films were measured by moving the stylus of Veeco Dektak Surface Profiler (150) across the film surface and across the film edge, respectively.

Results and Discussion

Figure 1(a) shows the chemical structure of P3HT molecule [41]. This structure repeats itself and forms long linear chains. P3HT is reported to exist in chains consisting of 100s to 1000s of such units repeating themselves. Figure 1(b) shows the basis of P3HT, when the polymers line-up to form a crystal structure (figure 1c). The distance between two lines of the thiophene structure gives the lattice parameter 'a' with the 'bc' plane being the reflecting plane for Bragg's diffraction. Inter-planar distance (d) works out to be equal to the lattice parameter 'a', resulting in the $2\theta \approx 5.2°$ diffraction maxima in XRD. The 'ac' plane shown in figure 1(c) repeats itself along the 'b'-direction, which is called the stacking direction. Such crystal structure of P3HT is referred too as 'edge-arrangement' [42]

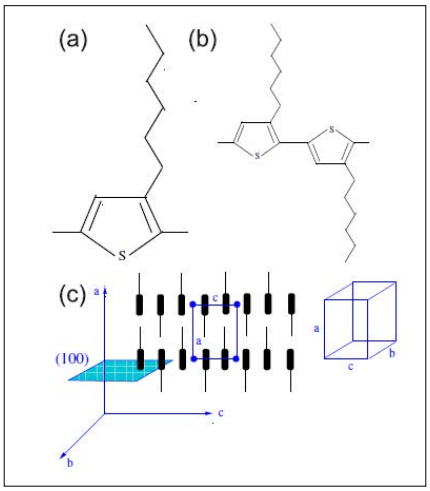

Figure 1: A single molecule of P3HT with a Thiophene Structure is shown in (a). Two such Molecules form the Basis Point for the Lattice (b). The Layer of Thiophene Molecules form the (100) Reflection Plane for X-rays. The $\pi - \pi$ Stacking is along the 'b'-Direction (c), which gives the Nano-Wire Crystal Structure.

Figure 2(a) exhibits the XRD pattern of P3HT films fabricated by spin coating at three different rpms as indicated in the figure. The films coated at the highest rotation speed showed a small minor peak at $2\theta \approx 5.2^{\circ}$, typical of the (100) popularly seen in literature. The samples grown at 6850 and 8150 rpm show several intense peaks. These peaks were indexed and the samples were found to have a tetragonal structure with lattice parameters, a ≈ 16.99Å and b=c ≈ 10.5Å. The lattice parameters are very similar to that reported by Poelking et al, expect that they had claimed the structure to be monoclinic with $\alpha \approx 86^{\circ}$. This suggests that there might be shear stress acting on the lattice of our samples [43]. This needs further investigation and will be discussed elsewhere.

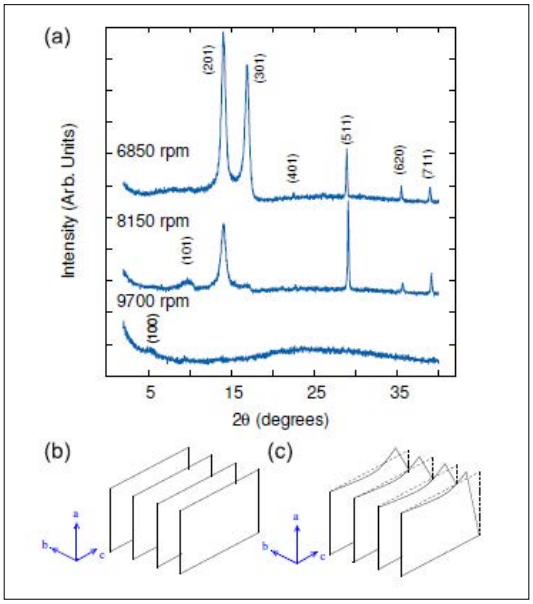

Figure 2: (a) Compares the Diffractograms of P3HT Films Grown by Spin Coating at Different rpms. (b) and (c) Compare How Centrifugal Force Assists in Edge-Stacking of the P3HT Layers. Figure Tries to Put Forward the Idea that Centrifugal Force Tends to Remove Any Twist or Kinks that might Appear in the Layers during Deposition.

In the sample fabricated at 9700 rpm, the intensity of the (100) peak is expectedly small, considering the high rpm would have resulted in a very thin coat of the film (Thinnest as measured and listed in Table 1). Along with this, considering that only a (100) diffraction peak was obtained, one can conclude that P3HT molecules were arranged in such a manner that the 'bc' lattice planes in this sample are co-planar with the substrate. This in turn implies that the lattice in this sample is highly oriented. The polymer chains would have been thrown in this orientation due to the high centrifugal forces acting on them because of high spinning speed during film formation, thus resulting in the 'bc' lattice planes to arrange themselves parallel to the substrate. Figure 2(b) shows $\pi - \pi$ stacking and formation of the nanowire along the 'c' direction. Since the film thickness is low, the number of reflecting-parallel 'bc' planes stacked would also be low, resulting in a minor diffraction maxima. In fact, in the Jimison et al study, where P3HT films were fabricated at 800 rpm, they observed that very thin films ($d \leq 40$ nm) were essentially disordered [44]. Thus, confirming our claim that the resulting centrifugal force at high rpm results in straightening of P3HT chains.

At slower rpms, the centrifugal force acting on the polymer chain can be appreciated as being lower, and hence the tension acting on the chain, stretching and pulling it into an oriented arrangement, would be lacking. Hence, one would expect that the 'ac' planes in the sample fabricated at 8150 rpm would develop a twist as shown in figure 2(c). This would expose more planes, other than the (100) plane, to the incident X-Rays, thus explaining more diffraction peaks. At 6850 rpm, the twists and hence deviation from oriented growth would be greater, resulting in more reflecting planes available for diffraction. This would explain the polycrystalline nature suggested by the XRD pattern. Normally in inorganic matter, the Full-Wdth at Half-Maxima (FWHM) of the XRD peaks would be a comment on the "grain size" or "ordering length" in the crystal structure. On the contrary, here in this study, the appearance of more diffraction peaks at lower rpms indicates a decrease in ordering (possibly more peaks are appearing with more twists or in other words, decreasing distance between two twists). Also, film properties of P3HT are usually explained by the bi-layer model [44]. As per this model, the P3HT film can be viewed as a bulk film with an interfacial layer, and ordering is easily achieved in the interfacial layer. As can be seen, lower rpm means a thicker film and hence a larger proportion of bulk region, making it more difficult to obtain oriented polymer chains.

Figure 3 compares the UV-visible spectrographs of all the samples grown at different rpms. The maximum intensities of the samples decreases with increasing rpm since the film thickness decreases. However, the main absorption peaks (between 450 and 650 nm) and their positions remain the same without exception. The inset of figure 3 shows the deconvolution of the broad peak of sample grown at 9700 rpm. The broad peak is a result of three overlapping absorption peaks lying at 480, 541 and the characteristic shoulder at 601 nm. The 480 nm peak is associated with the intra-chain $\pi - \pi^*$ transition of the thiophene rings (along 'a' and/or 'c' direction) and the higher wavelength peaks, 541 and 601 nm are associated with the inter-chain (between stacks along 'b' direction) interactions [45].

Table 1: The Variation in Film Thickness and Roughness w.r.t. Spin Speed

Spin Speed (rpm)	d (nm)	roughness (nm)
6850	120	20
8150	85	10
9700	40	10

However, in context with this study, it is the 680 nm peak that is of interest. The peak at 680 nm is not commonly observed. Rahimi et. al. have reported observing an absorbance peak around 680-700 nm in their study. This peak was intense in single crystal samples of size 59 nm and insignificant in 65 nm thin films [46]. The existence of this peak in our samples fabricated at 8150 and 9700 rpm corroborate our conclusion of ordering in 8150 and 9700 rpm samples from XRD analysis.

Clearly, all three samples have a certain amount of ordering and $\pi - \pi$ stacking (along the 'b' direction, as understood from our XRD results); however, as is evident from the occurrence of the 680 nm peak, samples grown at high rpms possess long range ordering. The centrifugal force ensures less twisting of the chains. More about this can be understood from the PL results of figure 4. Considering P3HT films show maximum absorption around 550 nm, the PL spectrographs were recorded using an excitation wavelength of 550 nm [47]. The sample fabricated at low speed exhibits typical PL spectrum of P3HT reported in literature with two peaks at 650 and 700 nm [48]. However, those grown at high speed show low yield with comparable area of the two peaks and a new peak at 743 nm. The low yield can be understood as a result of films having a lower thickness, also shown by decreased absorption in figure 4.

The more intense peak at ≈ 655 nm belongs to the 0-0 transition, while the less intense peak at ≈ 700 nm correspond to the 0-1 transitions. The origin of 0-0 peak is explained by transition of π-electrons between energy levels arising due to orbital overlap between adjacent thiophene rings of P3HT, i.e. inter-chain transitions [49-51]. On the other side, the 0-1 peak corresponds to the intra-chain transitions occurring between the energy levels of the same polymer chain. The high intensity of 0-0 emission as compared to that of 0-1 peak (in samples 1 and 2) is an indication of the overlap, existing due to folding and random arrangement of P3HT chains, with large disorder in the arrangement of P3HT polymer chains.

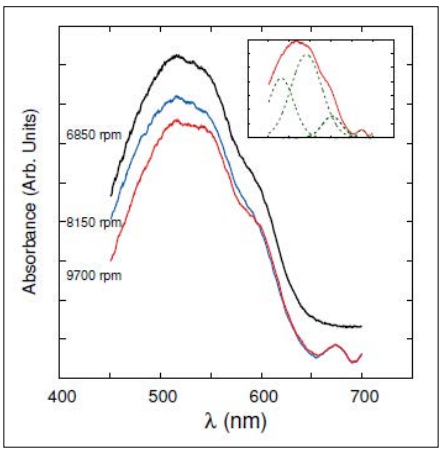

Figure 3: The Figure Compares the UV-Visible Absorption Spectra of Three Samples Grown at Different Spin Speeds. Spin Speeds are Indicated in the Figure. Inset Shows that Peaks are the Cumulative Effect of Three Absorption Peaks Appearing Very Close to Each Other.

Assuming the Huang-Rhys factor to be unity, the disorder (or ordering) in H-aggregate polymer chains has been quantified by the relation

$$\frac{A_{0-0}}{A_{0-1}} \propto \left(\frac{1 - \frac{0.24W}{E_p}}{1 + \frac{0.073W}{E_p}} \right)^2 \qquad (1)$$

where area ratio of the vibronic 0-0 transition (A_{0-0}) to the 0-1 transition (A_{0-1}) are compared [52]. We have assumed our samples to be H-aggregates since the crystal structure of our samples are tetragonal [53]. 'W' in eqn 1 is related to the exciton bandwidth and E_p is the energy of the intra-molecular vibrational mode (A_{0-0}) that is coupled to the electronic transition (A_{0-1}). The standard value of E_p for P3HT is given as 180 meV (location of our first to peaks in Figure 4 gives $E_p \approx 170$ meV) [54]. Table 2 lists the calculated values of 'W' for our samples depicted in Figure 2.

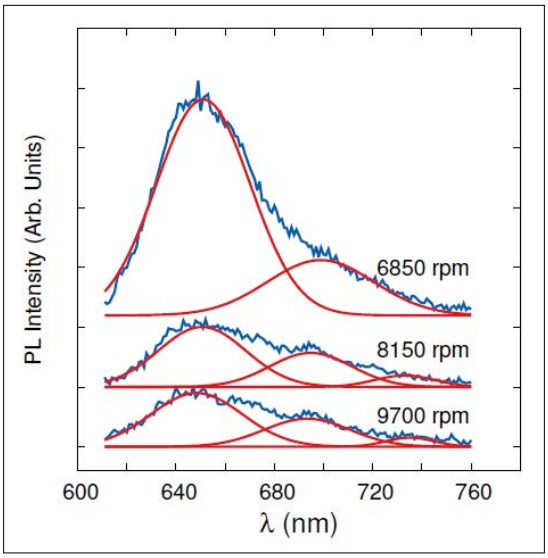

Figure 4: The PL Spectra of the Three Samples are Typically those of P3HT Reported in the Literature. However, a Third Peak at 743 nm is Visible in Samples made at 8150 and 9700 rpm.

Table 2: Table Lists the Area under the Curve for the Three Samples and use it to Calculate 'W' (also listed).

Sample (rpm)	A_{0-0}	A_{0-1}	W
6850	834	262	14.31
8150	210	102	5.71
9700	225	119	4.84

The value of 'W' is large for the film grown at low speed, while it is quite low for the films grown at high speed. It is well established that the intra-molecular ordering is inversely proportional to the magnitude of 'W', i.e.

$$intra - molecular\ ordering \propto \frac{1}{W} \qquad (2)$$

Hence, it would suggest that the polymer chains in samples grown at high speed are most likely straight, with no folding or bending. Also, decreasing 'W' with increasing spin rate would possibly mean a increase in P3HT polymer's intra-chain order. Thus, we believe P3HT's ability to coil and "imprison" PCBM molecule would decrease with increasing spin rate. This in turn would result in unstable hetrojunctions which would lead to rapid ageing of these solar cells. Further, the blue shift of ≈ 4 nm (≈ 0.014 eV) was seen in the 0-1 peak of films grown at higher speed. The blue shift is associated with reduced intermolecular interaction, which in turn would suggest that at high speed, the distance between P3HT molecules is increasing [55]. Finally, a new peak at 734 nm (1.69 eV) is seen that corresponds to the rarely reported 0-2 transition [56]. This is the vibrational mode associated with the second neighboring phonon w.r.t. the reference oscillator/phonon, thus further proving an increased ordering of P3HT chains in films grown at high spin rates [53]. Thus, all our analysis (XRD, UV-visible and PL) all point towards the same conclusion: films grown at high spin rate encourage the straightening and ordering of P3HT polymers.

P3HT: PCBM bulk heterojunction solar cells hold promise as a commercial device for the future. However, as recent works have shown, their junctions deteriorate very rapidly due to PCBM grains moving away for P3HT chains towards the film surface [57]. It is well known that P3HT molecules exist in coiled state. One would expect a coiled P3HT molecule would retain a PCBM cluster better and prevent disassociation of the two, thereby preventing rapid deterioration of the junction. Hence, from the above results it is evident that P3HT: PCBM films should be fabricated at very low spin speeds. To this extent, this group has started work in this direction. We have showed solar cells of P3HT: PCBM fabricated at a high speed of 8150 rpm deteriorate within hours of fabrication [58]. Work at lower spin-coating speeds is underway and will be reported elsewhere.

Conclusion

In the present work, three samples of P3HT films on glass substrates at different spin rates have been prepared. The centrifugal force seems to be the driving force behind the ordering of the polymer chains, which results in unfolding of the chains free from twists and kinks leading to formation of crystalline P3HT samples. The formation of crystalline structure has been confirmed by the occurrence of an additional tell-tale peak at 680-700 nm in the absorption spectrum along with a peak in the PL spectrum. Finding of this investigation argue that for obtaining a stable bulk-heterojunction sample of P3HT: PCBM solar cells with effecting coiling of P3HT polymer to hold PCBM molecules, fabrication should be done at very low spin speeds.

Data Availability: Data will be made available on request.

Statement on Conflict of Interest: The authors declare that they have no known competing financial interests or personal relationships that could have appeared to influence the work reported in this paper.

References

1. Liu W, Xie R, Zhu J, Wu J, Hui J, et al. (2022) A temperature responsive adhesive hydrogel for fabrication of flexible electronic sensors. npj Flex Electron 6: 1-10.
2. Lan L, Chen J, Wang Y, Li P, Yu Y, et al. (2022) Facilely accessible porous conjugated polymers toward high-performance and exible organic electrochemical transistors. Chem Mater 34: 1666-1676.
3. Wang Y, Li Z, Niu K, Xia W (2022) Energy renormalization for coarse-graining of thermomechanical behaviors of conjugated polymer. Polymer 256: 125159.
4. Gautam K, Singh I, Bhatnagar R, Bhatnagar PK, Peta KR (2022) Synergistic effect of graphene and ZnO nanorods in enhancing the performance of MEH-PPV based polymer light emitting diode. Displays 73: 102170.

5. Lee S, Kim H, Kim Y (2022) Lewis Acid-Doped Conjugated Polymer Nanolayers for Efficient Hole Injection in Phosphorescent Organic Light-Emitting Devices. ACS Appl Polym Mater 4: 6817.
6. Kazerouni N, Melenbrink EL, Das P, Thompson BC (2021) Ternary Blend Organic Solar Cells Incorporating Ductile Conjugated Polymers with Conjugation Break Spacers. ACS Appl Polym Mater 3: 3028-3037.
7. Lee Y, Mongare A, Plant A, Ryu D (2021) Strain-Microstructure-Optoelectronic Inter-Relationship toward Engineering Mechano-Optoelectronic Conjugated Polymer Thin Films. Polymers 13: 935.
8. Hsu F, Lin Y, Li C (2021) Stable polymer solar cells using conjugated polymer as solvent barrier for organic electron transport layer. Organic Electronics 89: 106008.
9. Sommer M (2021) 2-Development of conjugated polymers for organic flexible electronics. Organic Flexible Electronics 2021: 27-70.
10. Munshi J, Chien T, Chenc W, Balasubramanian G (2020) Elasto-morphology of P3HT: PCBM bulk heterojunction organic solar cells. Soft Matter 16: 6743.
11. Jana B, Bhattacharyya S, Patra A (2015) Conjugated polymer P3HT-Au hybrid nanostructures for enhancing photocatalytic activity. Phys Chem Chem Phys 17: 15392.
12. Sharma S, Singh I, Natasha, Kapoor A (2016) Effect of yttrium doping on structural and optical properties of zinc sulfide nanoparticles. Materials Science in Semiconductor Processing 56: 174.
13. Landgrave-Barbosa F, Marmolejo-Valencia AF, Baray-Calderon A, Hu H, Aguilar- Cordero JC, et al. (2022) Impact of thickness of spincoated P3HT thin films, over their optical and electronic properties. J Solid State Electrochemistry 26: 649.
14. Ren H, Tong Y, Ouyang M, Wang J, Zhang L, et al. (2022) Balancing the trade-off between the mechanical and electrical properties of conjugated polymer blend films for organic field-effect transistors. J Mater Chem C 10: 14921.
15. Zhang C, Yao H, Huang G, Wang X, Qiu L (2021) Tensile properties of two-dimensional poly (3-hexyl thiophene) thin films as a function of thickness. J Mater Chem C 9: 15065.
16. Wang GJN, Gasperini A, Bao Z (2018) Stretchable Polymer Semiconductors for Plastic Electronics. Adv Electron Mater 2018: 1700429.
17. Gostkowska-Lekner N, Kojda D, Hoffmann J, May M, Huber P, et al. (2022) Synthesis of organic-inorganic hybrids based on the conjugated polymer P3HT and mesoporous silicon. Microporous and Mesoporous Materials 343: 112155.
18. Suresh DS, Vandana M, Veeresh S, Ganesh H, Nagaraju YS, et al. (2022) Low-Cost Synthesis and Characterization of Donor P3HT Polymer for Fabrication of Organic Solar Cell. Materials Science and Engineering 1221: 012060.
19. Proscovia K, Cheon HJ, Shin SY, Jeong G, Go S, et al. (2022) Enhanced charge transport of conjugated polymer/reduced graphene oxide composite films by solvent vapor pre-treatment. Funct Compos. Struct 4: 025002.
20. Changa C, Paia C, Chena W, Jenekhe SA (2005) Spin coating of conjugated polymers for electronic and optoelectronic applications. Thin Solid Films 479: 254-260.
21. Quan L, Lee SS, Kalyon DM (2021) Dynamics of the sub-ambient gelation and shearing of solutions of P3HT and P3HT blends towards active layer formation in bulk heterojunction organic solar cells. Soft Matter 17: 1642.
22. Botiz I (2023) Prominent processing techniques to manipulate semiconducting polymer microstructures. J Mater Chem C 11: 364-405.
23. Yoon B, Ham D, Yarimaga O, An H, Lee CW, et al. (2011) Inkjet Printing of Conjugated Polymer Precursors on Paper Substrates for Colorimetric Sensing and Flexible Electro thermo chromic Display. Adv.Mater 23: 5492.
24. Ghosekar IC, Patil GC (2021) Review on performance analysis of P3HT: PCBM-based bulk heterojunction organic solarcells. Semicond Sci Technol 36: 045005.
25. Dixit SK, Madan S, Madhwal D, Kumar J, Singh I, et al. (2012) Bulk heterojunction formation with induced concentration gradient from a bilayer structure of P3HT: CdSe/ZnS quantum dots using inter-diffusion process for developing high efficiency solar cell. Organic Electronics 13: 710.
26. Thomas A, Tom AE, Ison VV (2022) An inverted architecture P3HT: CdSe bulk-heterojunction hybrid solar cell utilizing a quantum junction with high open circuit voltage and efficiency. Energy Reports 8: 12979.
27. Caldiran Z (2021) Fabrication of bulk heterojunction organic photovoltaic and effect of buffer layer on the basic solar cell parameters. Materials Today: Proceedings 46: 6929.
28. Subramanyam BVRS, Mahakul PC, Sa K, Raiguru J, Alam I, et al. (2021) Applications of carbon nanotubes in different layers of P3HT: PCBM bulk heterojunction organic photovoltaic cells. Materials Today: Proceedings 39: 1862.
29. Singh I, Bhatnagar PK, Mathur PC, Kaur I, Bharadwaj LM, et al. (2008) Optical and electrical characterization of conducting polymer-single walled carbon nanotube composite films. Carbon 46: 1141.
30. Qi Q, Zhong Y, Liu Y, Gao M, Peng Z, et al. (2022) Revealing the Molar Mass Dependence on Thermal, Microstructural, and Electrical Properties of Direct Arylation Polycondensation Prepared Poly(3-hexylthiophene). ACS Appl Polym. Mater 4: 1826.
31. Mkawi EM, Al-Hadeethi Y, Bazuhair RS, Yousef AS, Shalaan E, et al. (2021) Fabricated Cu2Zn SnS4 (CZTS) nanoparticles as an additive in P3HT: PCBM active layer for efficiency improvement of polymer solar cell. J Luminescence 240: 118420.
32. He J, Liu Y, Liu F, Zhou J, Huo H (2021) Roles of solution concentration and shear rate in the shear-induced crystallization of P3HT. RSC Adv 11: 19673.
33. Kumari A, Singh I, Prasad N, Dixit SK, Rao PK, et al. (2014) Improving the efficiency of a poly(3-hexylthiophene)-CuInS2 photovoltaic device by incorporating graphene nanopowder. Journal of Nanophotonics 8: 083092.
34. Deng H, Xiao M, Chai Y, Yuan R, Yuan Y (2022) P3HT-PbS nanocomposites with mimicking enzyme as bi-enhancer for ultrasensitive photocathodic biosensor. Biosensors and Bioelectronics 197: 113806.
35. Mousavi SL, Jamali-Sheini F, Sabaeian M, Cit RY (2021) Correlation of Physical Features and the Photovoltaic Performance of P3HT: PCBM Solar Cells by Cu-Doped SnS Nanoparticles. J Phys Chem C 125: 15841.
36. Ko S, Hoke ET, Pandey L, Hong S, Mondal R, et al. (2012) Controlled Conjugated Backbone Twisting for an Increased Open-Circuit Voltage while Having a High Short-Circuit Current in Poly(hexylthiophene) Derivatives. J Am Chem Soc 134: 5222.
37. Ghosh R, Luscombe CK, Hambsch M, Mannsfeld SCB, Salleo A, et al. (2019) Anisotropic Polaron Delocalization in Conjugated Homopolymers and Donor-Acceptor Copolymers. Chem Mater 31: 7033.
38. Seisembekova TE, Aimukhanov AK, Zeinidenov AK,

Ilyassov BR (2022) Competitive charge transport processes in inverted polymer solar cells based on ZnO thin films. Applied Physics A 128: 407.

39. Sudakov I, Landeghem MV, Lenaerts R, Maes W, Doorslaer SV, et al. (2020) The Interplay of Stability between Donor and Acceptor Materials in a Fullerene- Free Bulk Heterojunction Solar Cell Blend. Adv Energy Mater 2020: 2002095.
40. Wadsworth A, Hamid Z, Kosco J, Gasparini N, McCulloch I (2020) The Bulk Heterojunction in Organic Photovoltaic, Photodetector, and Photocatalytic Applications. Adv Mater 32: 2001763.
41. Bockmann M, Schemme T, de Jong DH, Denz C, Heuer A, et al. (2015) Structure of P3HT crystals, thin films, and solutions by UV/Vis spectral analysis. Phys Chem Chem Phys 17: 28616-28625.
42. Xing F, Su-Ling Z, Yu C, Jie Z, Qian-Qian Y,et al. (2015) Nano structure evolution in P3HT:PC61BM blend films due to the effects of thermal annealing or by adding solvent. Chinese Physics B 24: 078401.
43. Poelking C, Andrienko D (2013) Effect of Polymorphism, Regioregularity and Paracrystallinity on Charge Transport in Poly(3-hexylthiophene) [P3HT] Nanofibers. Macromolecules 46: 8941.
44. Jimison LH, Himmelberger S, Duongm DT, Rivnay J, Toney MF, et al. (2013) Vertical confinement and interface effects on the microstructure and charge transport of P3HT thin films. J Polym Sci B: Polym Phys 51: 611-620.
45. Park YD, Lee SG, Lee HS, Kwak D, Lee DH, et al. (2011) Solubility-driven polythiophene nanowires and their electrical characteristics. J Mater Chem 21: 2338.
46. Rahimi K, Botiz I, Agumba JO, Motamen S, Stingelin N, et al. (2014) Light absorption of poly(3-hexylthiophene) single crystals. RSC Adv 4: 11121.
47. Singh I, Bhatnagar PK, Mathur PC, Kaur I, Bharadwaj LM, et al. (2008) Optical and electrical characterization of conducting polymer-single walled carbon nanotube composite films. Carbon 46: 1141.
48. Bakour A, Bajjou O, Baitoul M, Massuyeau F, Wery J, et al. (2021) A study of the temperature effect on photoluminescence of the P3HT/MWNT nanocomposites. J Materials Today: Proceedings, Elsevier 36: 549.
49. Herrmann K, Freund S, Eller F, Robler T, Papastavrou G, et al. (2022) Microstructural and Thermal Transport Properties of Regioregular Poly(3-hexylthiophene-2,5-diyl) Thin Films. Materials 15: 7700.
50. Beer P, Reichstein PM, Schotz K, Raithel D, Thelakkat M, et al. (2021) Disorder in P3HT Nanoparticles Probed by Optical Spectroscopy on P3HTb- PEG Micelles. J Phys Chem A 125: 10165.
51. Baghgar M, Labastide JA, Bokei F, Hayward RC, Barnes MD (2014) Effect of Polymer Chain Folding on the Transition from H- to J-Aggregate Behavior in P3HT Nanofibers. J Phys Chem C 118: 2229.
52. Hestand NJ, Spano FC (2018) Expanded Theory of H- and J-Molecular Aggregates: The Effects of Vibronic Coupling and Intermolecular Charge Transfer. Chem Rev 118: 7069.
53. Yamagata H, Spano FC (2012) Interplay between intrachain and interchain interactions in semiconducting polymer assemblies: The HJ-aggregate model. J Chem Phys 136: 184901.
54. Kabongo GL, Mbule PS, Mhlongo GH, Mothudi BM, Hillie KT, et al. (2016) Photoluminescence Quenching and Enhanced Optical Conductivity of P3HTDerived Ho3+-Doped ZnO Nanostructures. Nanoscale Res Lett 11: 418.
55. Cannon JP, Bearden SD, Gold SA (2010) Characterization of conjugated polymer/anodic aluminum oxide nanocomposites fabricated via template wetting. Composites: Part A 41: 836.
56. Spano FC, Clark J, Silva C, Friend RH (2009) Determining exciton coherence from the photoluminescence spectral line shape in poly(3-hexylthiophene) thin films. J Chem Phys 130: 074904.
57. Berriman GA, Holmes NP, Holdsworth JL, Zhou X, Belcher WJ, et al. (2016) A new model for PCBM phase segregation in P3HT: PCBM blends. Organic Electronics 30: 12.
58. Mounika T, Belagali SL, Singh I, Kumar K, Arun P (2023) An Experimental Insight into the Reasons for Deterioration of P3HT: PCBM Bulk Heterojunction Solar Cells.Applied Solar Energy 59: 410.